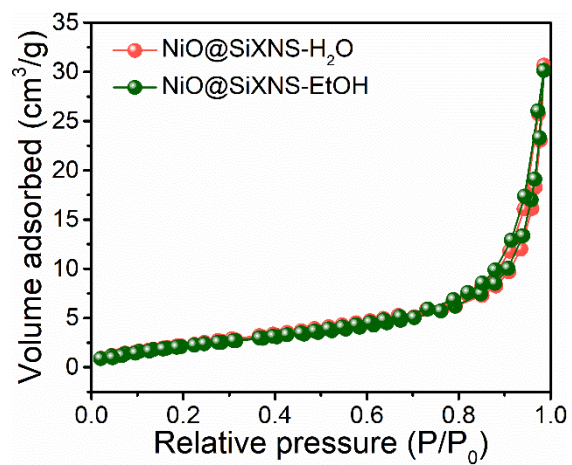


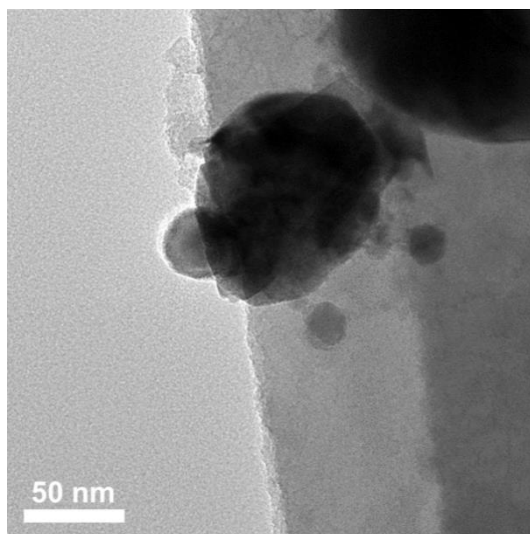
# Supplementary Information

## **Nickel@Siloxene Catalytic Nanosheets for High-Performance CO<sub>2</sub> Methanation**

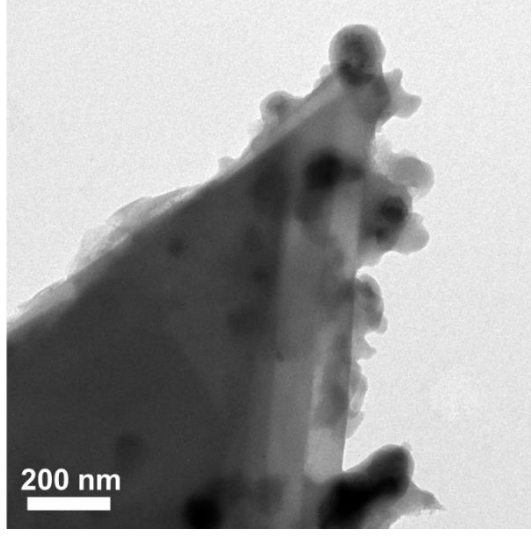
Xiaoliang Yan, Geoffrey A. Ozin



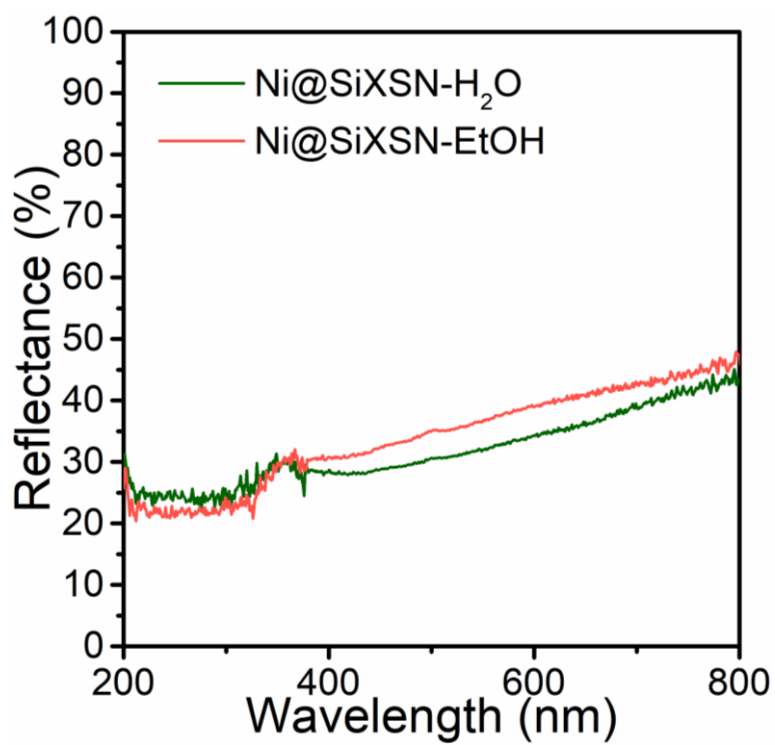
Supplementary Fig. 1. N<sub>2</sub> adsorption-desorption type III isotherms for NiO@SiXNS samples.



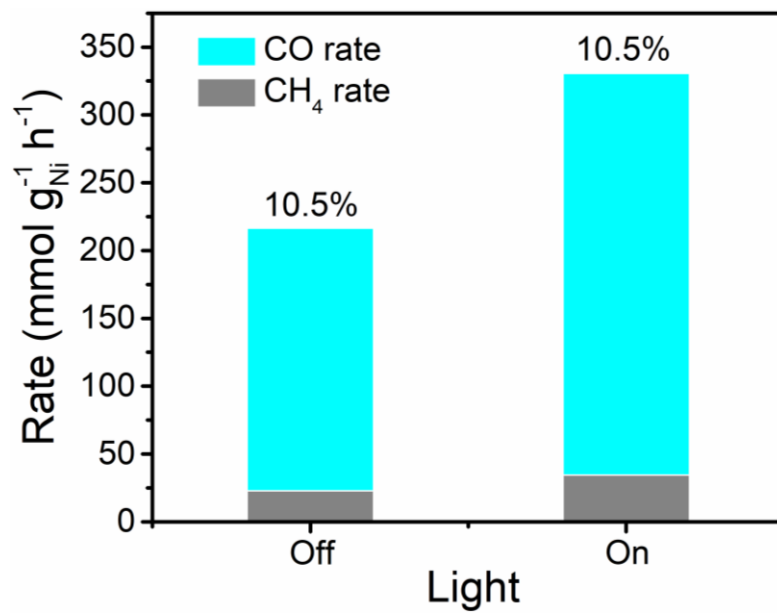
Supplementary Fig. 2. Representative TEM image of Ni@SiXNS-H<sub>2</sub>O.



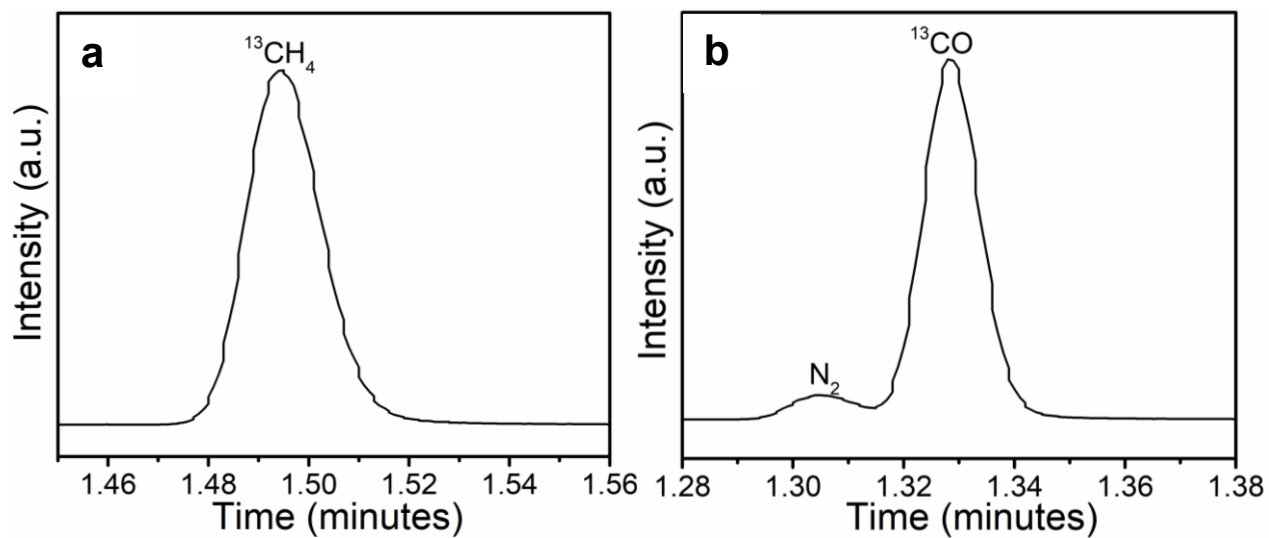
Supplementary Fig. 3. TEM image of Ni@SiXNS-EtOH captured at the edge of the composite material.



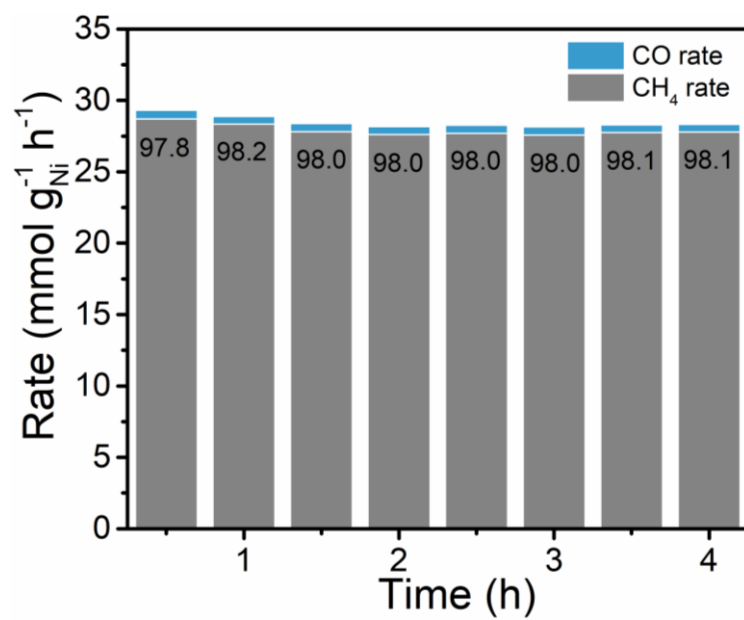
Supplementary Fig. 4. UV-vis diffuse reflectance spectra of Ni@SiXNS-H<sub>2</sub>O and Ni@SiXNS-EtOH.



Supplementary Fig. 5. The performance of hydrogenation of CO<sub>2</sub> to methane on Ni@SiO<sub>2</sub>.

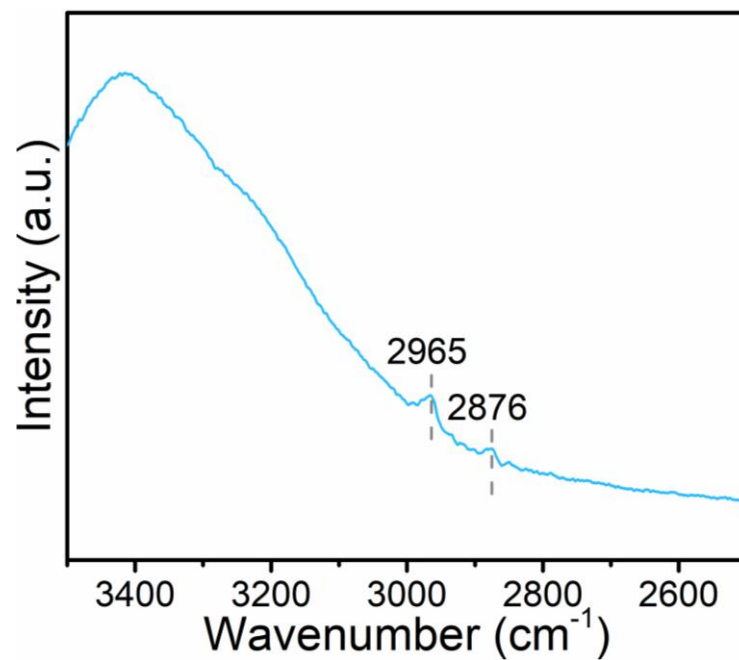


Supplementary Fig. 6. Mass spectra showing the ion mass (a) 17 and (b) 29 peaks for the  $^{13}\text{CO}_2$  methanation in light over Ni@SiXNS-EtOH, confirming the products are from conversion of  $^{13}\text{CO}_2$  input.

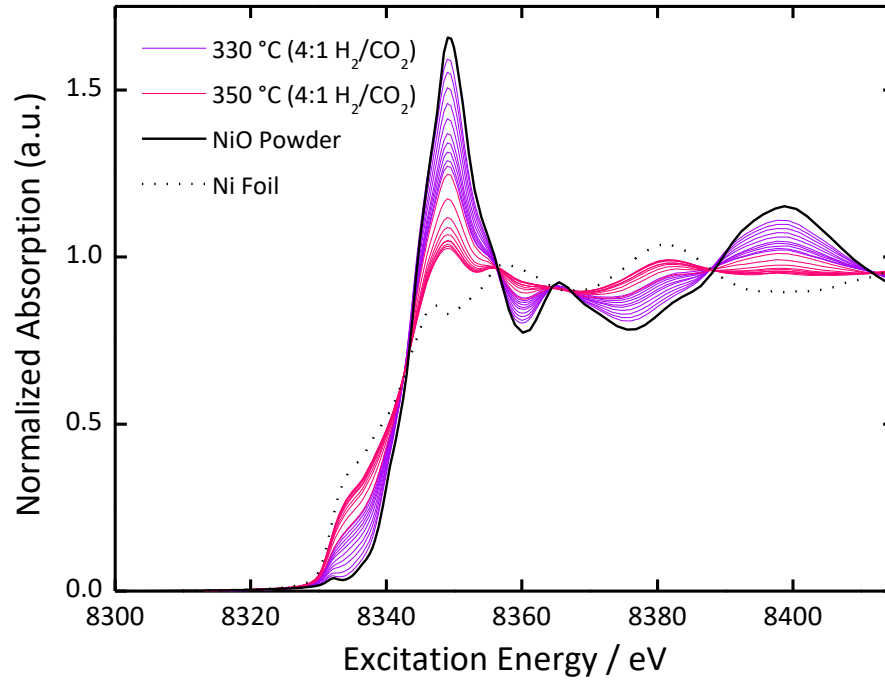


Supplementary Fig. 7. Catalyst test results for the hydrogenation of CO<sub>2</sub> on commercial 10 wt% Ni@Al<sub>2</sub>O<sub>3</sub>.

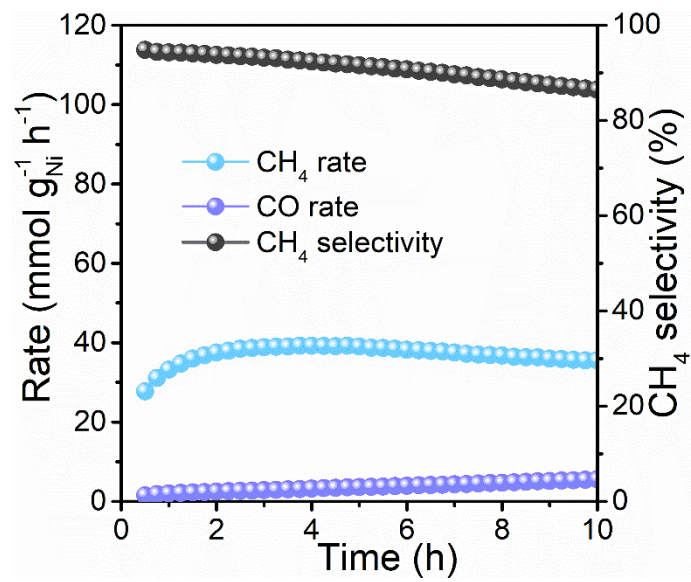




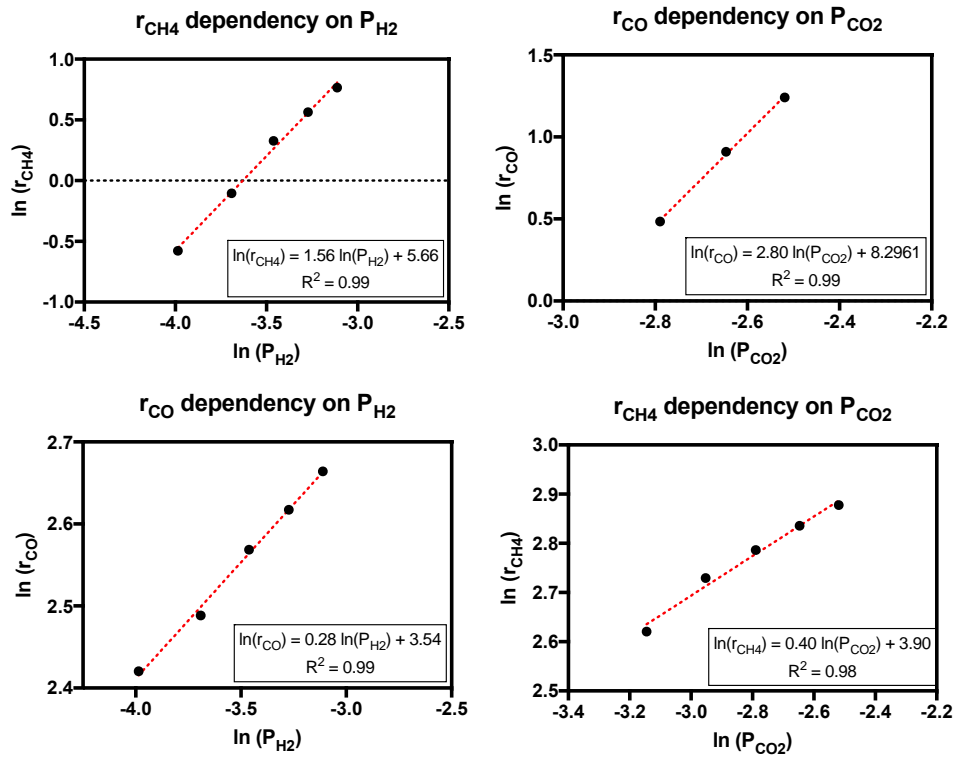
Supplementary Fig. 8. DRIFTS spectrum of Ni@SiXNS-EtOH showing two discernible peaks of C-H mode in HCOOH, acquired after performing *in-situ* CO<sub>2</sub> methanation for 60 min, followed by rapid cooling to 30 °C.



Supplementary Fig. 9. EXAFS spectra acquired at the Ni K-edge of the NiO@SiXNS-EtOH sample at different reaction temperatures with Ni foil and NiO powder reference.



Supplementary Fig. 10. Rapid stabilization of CO<sub>2</sub> methanation by pre-treating the sample with H<sub>2</sub> at a slightly higher temperature of 350 °C and subsequently exposing it to CO<sub>2</sub> and H<sub>2</sub> at 300 °C for 10 h.



Supplementary Fig. 11. Derived from the rate law  $r = kP_{H_2}^a P_{CO_2}^b$ , the function  $\ln(r) = \ln(k) + a \ln(P_{H_2}) + b \ln(P_{CO_2})$  is plotted to determine reaction orders versus partial pressures of  $H_2$  and  $CO_2$ , keeping one fixed and the other varied.

## Supplementary Notes

### Rate Law Analysis:

Stoichiometric analysis of the parallel reaction network for CO<sub>2</sub> conversion to either CO or CH<sub>4</sub> provided the following relationships between the species in the system that were measured (CO and CH<sub>4</sub>), and those that were not directly measured:  $r_{CO_2} = r_{CO} + r_{CH_4}$ ,  $r_{H_2} = r_{CO} + 4r_{CH_4}$ , and  $r_{H_2O} = -r_{CO} - 2r_{CH_4}$ .

Based on this, the rates of all species in the system were calculated, as well as the fractional yields (s) for both CH<sub>4</sub> and CO from CO<sub>2</sub> were calculated. Results can be seen in the table below.

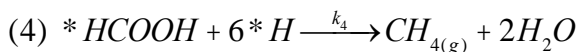
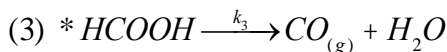
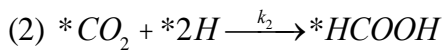
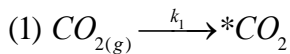
Table 1. The rates of all species in CO<sub>2</sub> methanation and the fractional yields for CH<sub>4</sub> and CO from CO<sub>2</sub>.

P <sub>H2</sub>	P <sub>CO2</sub>	r <sub>CH4</sub>	r <sub>CO</sub>	r <sub>CO2</sub>	r <sub>H2</sub>	r <sub>H2O</sub>	S <sub>CH4/CO2</sub>	S <sub>CO/CO2</sub>
0.018	0.250	0.561	0.025	-0.587	-2.271	-1.148	0.957	0.043
0.024	0.250	0.901	0.261	-1.162	-3.865	-2.063	0.775	0.224
0.031	0.250	1.389	0.700	-2.089	-6.254	-3.477	0.665	0.335
0.037	0.250	1.759	0.233	-1.992	-7.268	-3.751	0.883	0.117

**As can be seen, S<sub>CH4</sub> > S<sub>CO</sub> for the entire range of feed compositions, indicating that the rate of formation of CH<sub>4</sub> production and the selectivity of CH<sub>4</sub> production from CO<sub>2</sub> are higher than that for CO.**

In the absence of experimental data to specifically determine each of the rate constants, the relative production or consumption rates of each species can be qualitatively examined to rationally determine the potential rate limiting step of this reaction system.

Stoichiometric analysis for the reaction pathway depicted in Fig. 6. produced a formula matrix that was inconsistent and underdetermined and therefore unsolvable. In order to remove these mathematical restrictions, steps (2) and (3) above can be combined to approximate a hybrid step that encompasses both the formation of the surface bound formate, and its subsequent combination with a surface hydride to produce a surface-bound formic acid molecule. The reaction network representing this approximated system then becomes:



Stoichiometric analysis of relationships between species for the reaction system:  $r_{*CO_2} = r_{CO_2} - 3r_{CH_4}$ ,  $r_{*H} = -r_{H_2O} + r_{CO} - 2r_{CH_4}$ , and  $r_{*HCOOH} = r_{H_2O} + 2r_{CH_4}$ .

$P_{H_2}$ (atm.)	$P_{CO_2}$ (atm.)	$r_{CH_4}$	$r_{CO}$	$r_{CO_2}$	$r_{H_2}$	$r_{H_2O}$	$r_{*CO_2}$	$r_{*H}$	$r_{*HCOOH}$
0.018	0.250	0.562	0.025	-0.587	-2.271	-1.148	-2.271	0.050	-0.025
0.024	0.250	0.901	0.261	-1.162	-3.865	-2.063	-3.865	0.522	-0.261
0.031	0.250	1.389	0.700	-2.089	-6.254	-3.477	-6.254	1.400	-0.700
0.038	0.250	1.759	0.233	-1.992	-7.268	-3.751	-7.268	0.467	-0.233

Looking at these results, we can make the following observations: as  $P_{H_2}$  in the system increases,

- $CH_4$  is produced at a faster rate
- $CO_2$  is consumed faster
- $H_2$  is consumed faster
- $*CO_2$  is consumed faster
- $*H$  species are produced at the same rate
- $CO$  is produced at the same rate, and
- $*HCOOH$  is consumed at the same rate

In principle, increasing the concentration of  $H_2$  in the feed should, by Le Chatelier's principle, push the equilibrium of reactions (1) to (4) towards their respective product production when the  $P_{H_2}$  in the feed is increased.

As can be seen from the rate results in the table above,  $*H$  is produced at the same rate when  $P_{H_2}$  in the feed is increased, therefore the generation of  $*H$  is not influenced by the increased concentration of  $H_2$  in the system. This could be because the following reaction step (3), the consumption of  $*HCOOH$  is also unchanged by the increased concentration of  $H_2$  in the feed, suggesting that the reaction system is "held up" by reaction (4), and the catalyst surface sites are not being vacated by  $*HCOOH$  at a rate that would make the surface sites available for the faster generation of  $*H$  species.

In contrast, the rate of  $CH_4$  production increases as  $P_{H_2}$  increases. This is in line with the expected equilibrium shift as a result of Le Chatelier's principle for the overall methanation reaction. We can also eliminate reaction (1) as the potential RDS as  $*CO_2$  species are shown to be consumed faster as  $P_{H_2}$  is increased.

Based on this analysis, we postulate that the RDS for  $CH_4$  production from  $CO_2$  is the final step in which  $*HCOOH$  reacts with a cluster of surface hydrides to desorb as  $CH_{4(g)}$ .